Lasers in Manufacturing Conference 2015

Energy transfer mechanisms during laser pulsed processing of metals

Daniel J. Förster[a,b,*], Duc Anh Bui[b], Volkher Onuseit[b], Rudolf Weber[b], Thomas Graf[b]

[a]*Graduate school of advanced Manufacturing Engineering, University of Stuttgart, Nobelstraße 12, 70569 Stuttgart*
[b]*Institut für Strahlwerkzeuge, University of Stuttgart, Pfaffenwaldring 43, 70569 Stuttgart*

Abstract

The basic behaviour of material removal rates in volume laser ablation processes when using ultra-short laser pulses can be described by simple models based on the Beer-Lambert law with an exponential decay of the energy density into the material of an externally applied laser field according to preliminary findings of J.H. Lambert, 1760 and A. Beer, 1852. Neuenschwander et al., 2014 showed that the use of different pulse lengths results in different “effective” penetration depths of energy into the material. At certain parameters, these are in the range of the optical penetration depth. However, for a wide range of pulse durations the effective penetration depth is much larger than the optical penetration depth. The reasons for this behaviour are several energy transfer mechanisms like photon-electron, electron-electron and electron-phonon interactions.

For short- and ultrashort-pulsed laser processing, wide-range two temperature model calculations for several pulse durations were carried out for aluminium. The simulations enable to distinguish between different energy transfer mechanisms. The influence of optical absorption and energy transport mechanisms for different pulse durations and applied fluences are discussed in the present paper.

Keywords: Energy transfer; Volume ablation; Two Temperature Model; Fundamentals of pulsed processing

* Corresponding author. Tel.: +49 711 685 69754.
E-mail address: daniel.foerster@ifsw.uni-stuttgart.de.

1. Introduction

Built upon investigations of Kaganov et al., 1957 and Anisimov et al. 1974, Chichkov et al. in 1996 applied the one dimensional, two-temperature diffusion model (TTM) on laser ablation processes of metals in the femto-, pico- and nanosecond pulse duration regime. In principal two diffusion equations – one for the electronic and another for the ionic system – are coupled via an energy exchange term. Electrons interacting with an external electromagnetic field are excited and able to transport energy within the electronic system into the material. The energy of the laser field is absorbed within the material according to the Beer-Lambert law, following an exponential decay with characteristic optical penetration depth α, at which e^{-1} of the surface energy density is reached. The electronic system exchanges energy with the ionic system, yielding to heating or direct bond braking processes. For both femtosecond and picosecond laser pulse durations, the basic figure of merit for material removal, the ablation depth, is

$$z_{abl} = \alpha^{-1} \ln(F/F_{th})$$

with F_{th} being the threshold fluence for significant evaporation, i.e. solid-vapor or solid-plasma phase transitions [Chichkov et al. 1996]. This formula directly follows from TTM equations when solving for the attainable lattice temperature T_i, following the dependence $T_i \sim \alpha \exp(-\alpha\, z)$. For longer pulses in the nanosecond regime, when the laser pulse duration highly exceeds the electron-phonon relaxation time, the TTM equations decompose into the classical heat conduction equation, governed by the heat penetration depth $l = \sqrt{D\, t}$ with heat diffusion coefficient D.

In the following, the numerical code Polly-2T of the Joint Institute of High Temperatures of the Russian Academy of Sciences (RAS), Moscow, Russia is used (online available as “Virtual Laser Lab” at http://vll.ihed.ras.ru/). A one dimensional two temperature model is coupled with Maxwell equations. Material hydrodynamic equations of aluminum are further used to more accurately consider the material answer to irradiation. Due to the transient nature of the processes involved, namely optical wave travelling, electronic absorption and electronic energy transfer, lattice heating and heat transfer as well as material reactions such as melting, evaporation and ionization, the basic models are extended and main figures of merit of energy transport mechanisms are deduced and investigated. We aim for a better understanding of changes in the optical penetration depth and absorption during pulse interaction.

2. Numerical method

The present results have been obtained through the use of Virtual Laser Laboratory (URL http://vll.ihed.ras.ru). It uses a wide-range model for laser matter interaction, i.e. a thermodynamically complete equation of state and radiation coupling by Maxwell equations. The code is developed by the Joint Institute for High Temperatures (RAS), Moscow and allows for the one dimensional simulation of laser ablation of different materials. Aluminum has been investigated and the model shows well accordance with standard ablation experiments but also more complex setups regarding pump-probe, phase transition and shock wave measurements [M. E. Povarnitsyn et al., 2007, M. E. Povarnitsyn et al., 2007, M. E. Povarnitsyn et al., 2009, M. E. Povarnitsyn et al., 2012].

The aluminum material is modelled by the use of discretized space domains with

- wave traveling according to Maxwell equations,
- taking into account the permittivity with an transition from a Drude-like model and plasma model below and beyond the Fermi-Energy, respectively,
- a hydrodynamic single fluid two-temperature material model,
- taking into account mass and momentum conservation of electrons and ions.

Further details are described in M. E. Povarnitsyn et al., 2012.

3. Simulation setup

The numerically irradiated aluminum targets are of 1mm thickness and surrounded by vacuum. Laser irradiation is linearly polarized at a wavelength of 1064 nm under normal incidence. The Gaussian shape in time domain reads

$$\mathrm{I}(t) = \mathrm{I}_0 \cdot \exp\left(-\frac{t^2}{2\cdot\tau^2}\right) \ ,$$

with full width half maximum (FWHM) pulse duration

$$\tau_{FWHM} = \sqrt{2\cdot\ln(2)}\cdot\tau$$

and peak intensity

$$\mathrm{I}_0 = \frac{\overline{\Phi}}{2.507\cdot\tau} \ ,$$

with mean fluence

$$\overline{\Phi} = \frac{E_{Pulse}}{\pi\cdot\omega_0^2} \ .$$

FWHM pulse durations are varied from 100 fs to 1 ns, whereas the applied mean fluence $\overline{\Phi}$ is varied from $0.1\ \mathrm{J/cm^2}$ to $18\ \mathrm{J/cm^2}$ in order to obtain material answers below and far above the ablation threshold (0.32 J/cm² for 12 ps [E. G. Gamaly, 2011], in house experiments 0.23±0.01 J/cm² for 10 ps). The simulation time begins at least three times the pulse duration before the pulse maximum, whereas the simulation time of 0 ps always correspond to the maximum applied fluence. Since the Maxwell equations are solved according to the permittivity distribution the incoming waves interact with, an effective optical penetration depth $\boldsymbol{\delta_{opt}}$ can be obtained. It is defined as the spatial distance from the initial surface at $z = 0$ to the z-position were the absolute value of the incoming wave $|E(z)|$ has decreased to e^{-1} of its initial value (cf. Figure 1 b). Additionally, by setting the absorbed energy in relation to the total input energy, an effective reflectivity R_{eff} can be defined. During irradiation, extension of the material and phase transitions may occur (cf. figure

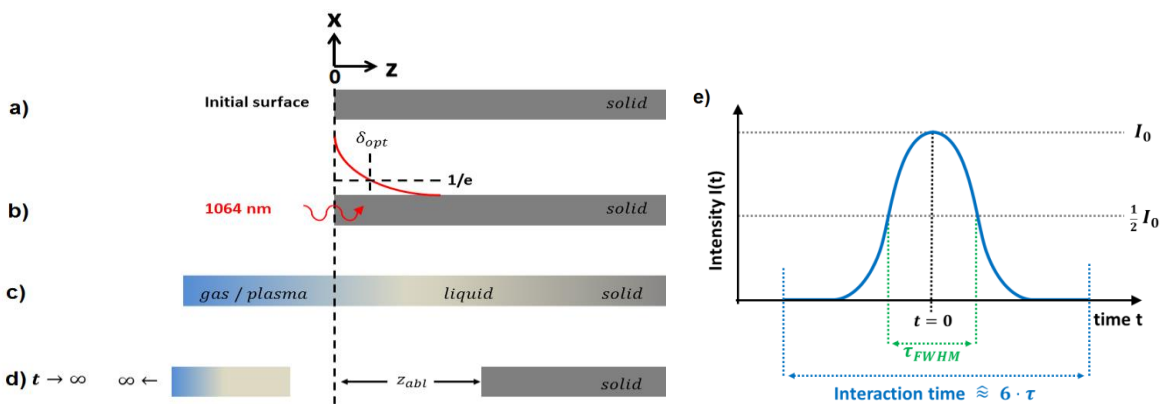

Figure 1. Involved processes in laser ablation (schematic) and definitions: a) initial surface, b) optical penetration depth definition, c) extension and phase transitions, d) Ablation depth definition after ablation, e) time scale definitions and figures of merit

1c). Finally, after the ablation process an ablation depth z_{abl} can be obtained from a new solid surface (cf. figure 1d). Since the total ablation process time lies in the range of several 100 nanoseconds or milliseconds, the ablation depth could not be obtained yet due to short simulation times.

4. Results and discussion

First we consider the changes of optical material properties. In Figure 2 on the left (figures a-d) for different pulse durations the temporally resolved reflectivity of the material during laser pulse irradiation is given. As can be seen, the reflectivity does only change slightly for fluences below or close to the ablation threshold (around 0.3 J/cm²). During ablation processes, the simulations show a high influence of fluence and pulse duration due to changes in the excitation of matter. For example, the reflectivity drops for 100 fs pulse duration during irradiation from about 94% to 84% for 0.78 J/cm² and to 65% after a downfall to 60% for 18.19 J/cm². For longer pulse durations, the reflectivity during the pulse even decreases to 0%. This happens for example 100ps after the pulse maximum during a 100ps pulse, as long as the fluence is higher than 0.78 J/cm².

Furthermore, the optical penetration depth δ_{opt} over time is given for different pulse durations in Figure 2, right column (figures e-h). At the beginning of irradiation, it lies constantly at 7 nm, while it increases slightly for 100 fs pulse duration to a few tens of nanometers. Interestingly, the maximum penetration depth stays the same for 5 and 18 J/cm², although the maximum is reached earlier in latter case. For longer pulse durations, at first a decrease of optical penetration depth can be observed. The material at the initial surface position is heated up and extends in the direction of the incoming radiation. Since the penetration depth is defined from the initial surface on, it is possible to decrease in this description. Beside this definition wise occurrence, the main cause of the global behavior, an increase of absorption and optical penetration depth, is due to the fundamental behavior of permittivity. Its value is dependent on laser wavelength, electron concentration and hence local density, as well as ionic and electronic temperature. In the apparent time scales, latter is the main influence parameter, together with electron concentration and density. Wavelength is constant in this publication and ionic temperature rises much slower than electronic. While the real part of the permittivity decreases with higher electron temperature, the imaginary part rises [M.E. Povarnitsyn et al. 2012]. In case of 100 fs pulse duration, this leads to an increase of optical penetration depth and absorption (cf. Figure 2 a),e)) for fluences higher than the ablation threshold. When the electronic system is saturated, absorption also saturates and the optical penetration depth does not rise further (around 10 fs for 18 J/cm² and 100 fs for 5 J/cm² after pulse maximum). From this time on material in a metastable solid-liquid state extends the initial surface (cf. Figure 5a)), resulting in a decrease of penetration depth. The electronic excitation also decreases due to increasing pulse energy, resulting in again increasing reflectivity.

For longer pulse durations, the effect of extending surface material is better visible. So e.g. the beginning of extension again corresponds well with a decrease in optical penetration depth at simulation time -5 ps for a 10 ps pulse of fluence 2.59 J/cm² (cf. Figure 2g) and Figure 5b)). The decrease ends at simulation time -2 ps when clear evaporation takes place. In the vapor absorption again drops and the material tends to absorb again closer to the initial surface and from simulation time -1 ps on even deeper. The optical penetration depth then saturates after a steep rise due to less incoming laser energy and hence less electronic excitation. The beginning of evaporation also shows an effect on reflectivity. While it decreases in the first time due to rising pulse energy and electronic excitation, the evaporation turns probably excitable material into non excitable (vapor). This results in a total reflectivity rise at simulation time -2 to 5 ps. Afterwards further material is liquefied and excitable than before, and reflectivity decreases again. This behavior holds also for longer pulse duration. The more material is electronically excited, the better absorption is.

Figure 2. Temporally resolved reflectivities (left column, a-d) and optical penetration depths (right column, e-f) during laser irradiation. Laser pulse durations are given on the right. The resolution of the time axis is 2% of pulse duration, e.g. 2 fs for 100 fs pulse duration

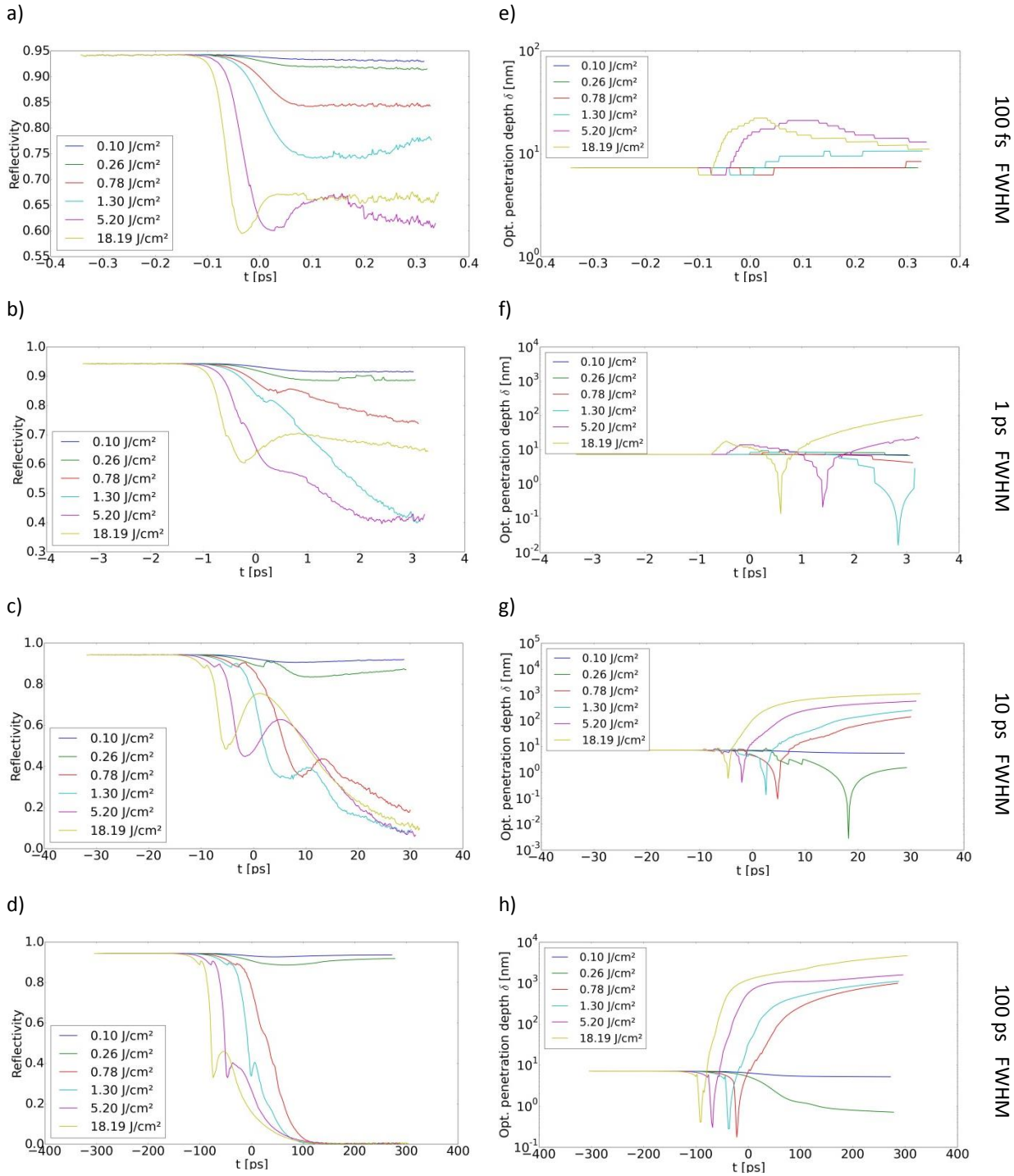

In Figure 3, an overview of the mean absorption

$$\overline{A} = 1 - \overline{R} = 1 - \frac{1}{6\tau} \int_{-3\tau}^{3\tau} R(t)\, dt$$

of every simulated pulse duration is given. During simulation time $t \in [-3\tau, +3\tau]$ radiation is applied and affects the target. As can be seen, for all pulse durations there occurs a steep increase of absorption from the standard textbook reflectivity of 6% for 1064 nm given by Fresnel equations to pulse duration dependent saturation values for fluences between 0.5 and 1 J/cm². In general, longer pulse durations lead to an increase of absorption.

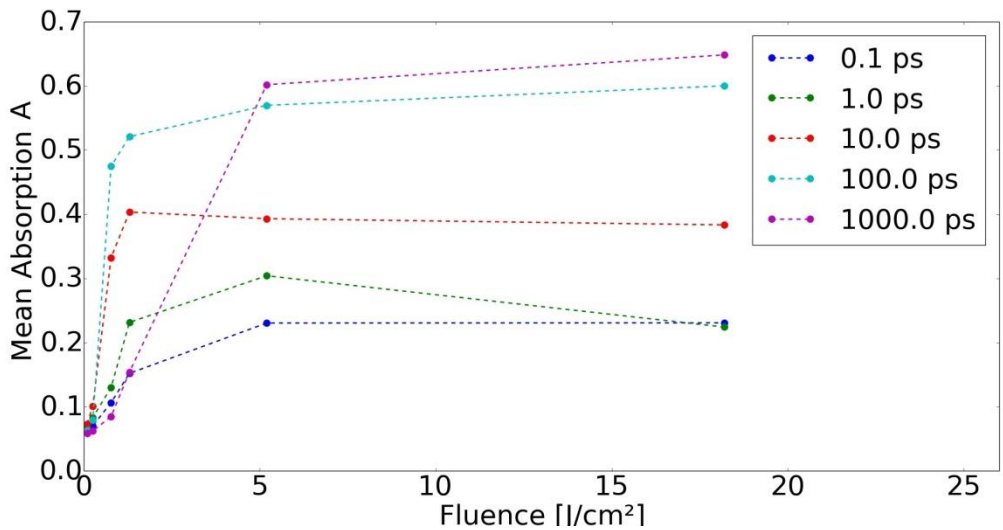

Figure 3. Averaged absorption for different pulse durations and fluences

An overview of optical penetration depths is given in Figure 4, where the averaged optical penetration depth

$$\overline{\delta_{opt}} = \frac{1}{6\tau} \int_{-3\tau}^{3\tau} \delta_{opt}(t)\, dt$$

is plotted. Also, in general, longer pulse durations increase the optical penetration depth. While for 100 fs and 1 ps pulse duration it stays in the range of the textbook absorption coefficient (8-20 nm, e.g. E. G. Gamaly, 2011), it increases about a factor of 20 for 10 ps (200-450 nm) and 3 to 4 for 100 ps (800-1200) and another factor of 5 for 1 ns (1500-6000). This results in the existence of an ideal pulse duration for optical energy input, since the transferred energy per depth changes. For standard two-temperature calculations in literature mostly a constant skin depth is used. It should be noted that for ultrashort pulses shorter than 1 ps this assumption according to our simulations is correct and is almost fluence independently in the range of the standard textbook optical penetration depth. However, for longer pulse durations up to 1 ns the optical penetration depth increases in factors of 10 to 400.

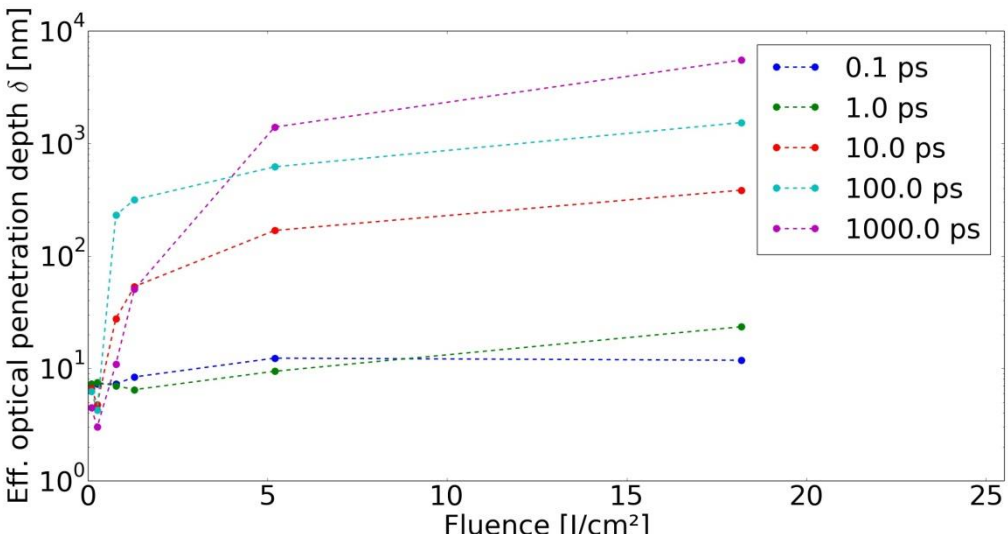

Figure 4. Averaged effective optical penetration depths for different pulse durations and fluences

Most of standard heat transfer and two temperature modelling approaches have shown to increase melt layer thickness, which is additionally amplified by the pure optical penetration presented in this paper.

Summarizing up the electromagnetic behavior when irradiating aluminum at 1064 nm wavelength with a single pulse, with increasing pulse duration the optical penetration gets higher and more laser energy is absorbed within the material. While energy absorption increases by a maximum factor of 7, the optical penetration depth increases up to a factor of 500. As implication, the energy per depth ratio decreases with longer pulse duration, leading to thicker melt films and less ablated material per pulse. For longer pulse durations than 100 fs, this increase in absorption happens within the material at the front, expanding further than the initial surface. During expansion, also melting and evaporation take place. The higher the applied fluence, the earlier evaporation occurs and the deeper the electronic excitations take place.

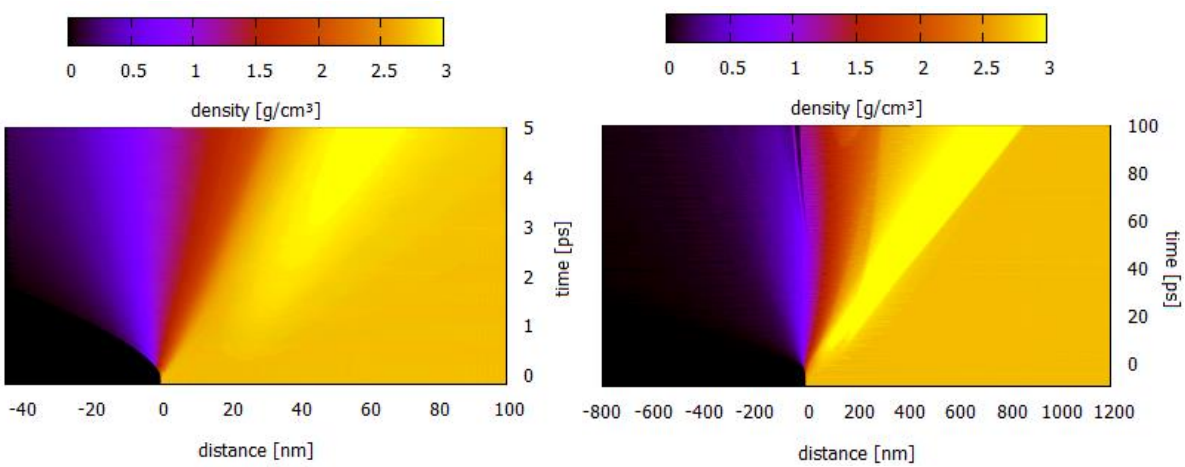

Figure 5. Density development in time and space for the 10ps before maximum fluence until 100ps after maximum fluence. Distance zero is the initial surface, pulse durations 100 fs (left) and 10 ps (right), solid density equals 2.712 g/cm³

5. Conclusion and outlook

In this paper, numerical investigations were performed in order to figure out the transient behavior of optical penetration depths and reflectivity during irradiation of short and ultrashort laser pulses on aluminum at 1064 nm. In conclusion, the longer the pulse duration and applied fluence, the higher the penetration depth and reflectivity gets.

In the future, detailed comparisons with experimental findings with respect to ablation depths, melt layer formation as well as electron and thermal penetration depths will be investigated closer.

Acknowledgements

The authors would like to thank Dr. S. Scharring from German Aerospace Center (DLR), Stuttgart and Dr. M. E. Povarnitsyn from the Russian Academy of Sciences (RAS), Moscow for fruitful discussions.

References

B. Neuenschwander et al., 2014, "Surface structuring with ultra-short laser pulses: Basics, limitations and needs for high throughput", 8th International Conference on Photonic Technologies LANE 2014, Physics Procedia 56, p. 1047 – 1058

J.H. Lambert, 1760, Photometria sive de mensura et gradibus luminus, colorum et umbrae

A. Beer, 1852, Bestimmung der Absorption des rothen Lichts in farbigen Flüssigkeiten. Annal. Phys. Chem. 86, p. 78–88

M.I. Kaganov, I.M. Lifshitz, L.V. Tanatarov, 1957, Sov. Phys.-JETP, 4, 173

S.I. Anisimov, B.L. Kapeliovich, T.L. Perelman, 1974, Sov. Phys.-JETP 39, 375

B.N. Chichkov, C. Momma, S. Nolte, F. yon Alvensleben, A. Tünnermann, 1996, Femtosecond, picosecond and nanosecond laser ablation of solids, Appl. Phys. A 63, p. 109-115

M. E. Povarnitsyn, T. E. Itina, K. V. Khishchenko, P. R. Levashov, 2007, Multi-material two-temperature model for simulation of ultra-short laser ablation, Applied Surface Science, Volume 253, Issue 15, pp. 6343–6346

M. E. Povarnitsyn, T. E. Itina, M. Sentis, K. V. Khishchenko, and P. R. Levashov, 2007, Material decomposition mechanisms in femtosecond laser interactions with metals, Phys. Rev. B 75, 235414

M. E. Povarnitsyn, K. V. Khishchenko, P. R. Levashov, 2009, Phase transitions in femtosecond laser ablation, Applied Surface Science, Volume 255, Issue 10, pp. 5120-5124

M. E. Povarnitsyn, N. E. Andreev, E. M. Apfelbaum, T. E. Itina, K. V. Khishchenko, O. F. Kostenko, P. R. Levashov, M. E. Veysman, 2012, A wide-range model for simulation of pump-probe experiments with metals, Appl. Surf. Sc., Vol. 258, Is. 23, pp. 9480-948

E. G. Gamaly, 2011, Femtosecond Laser-Matter Interaction: Theory, Experiments and Applications, Pan Stanford